

COMPARISON OF ASSOCIATED AND NON-ASSOCIATED PLASTICITY MODELS FOR ALUMINIUM ALLOYS

Vobejda R.^{*}, Šebek F.^{**}

Abstract: A great deal of products are made from steel sheets, which often exhibit anisotropic behaviour. It is necessary to capture this phenomenon in the design stage to obtain reliable predictions and effective manufacturing. Two different models are compared for two aluminium alloys, 6022-T4 and 2090-T3. The role of associativity and non-associativity is studied with respect to the predictability of yield stresses and r -values.

Keywords: Flow, Hardening, Lankford, Orthotropy, Plate.

1. Introduction

Sheets of metal are often produced by cold or hot rolling, when the grains are severely deformed. This leads to a thin anisotropic material where plane stress condition prevails. Then, it can be used for further processing like stamping parts for the automotive or aerospace industry.

2. Calibration of two plasticity models for two aluminium alloys

The main advantage of models that use directional distortional hardening is the ability to capture the evolution of the yield surface with increasing strain, while the calibration remains simple. This is due to yield stresses appearing directly in the yield condition, while being functions of plastic multiplier. There are typically yield stresses from tensile tests in 0° , 45° and 90° directions with respect to rolling, σ_0 , σ_{45} and σ_{90} , respectively, and yield stress for equi-biaxial tension, σ_{EB} . Then, the plastic potential is not coupled with the yield function in any way, and its calibration is mostly carried out based on the Lankford coefficients (r -values) determined from the tensile tests in 0° , 45° and 90° directions with respect to rolling, r_0 , r_{45} and r_{90} , respectively. Most of the models use the plastic potential as a quadratic function according to Hill (1948), where the Lankford coefficients are directly present. Min et al. (2016) proposed a function for the plastic potential that allows for the inclusion of the Lankford coefficient for the equi-biaxial tension, r_{EB} . Unfortunately, the Lankford coefficients are not directly present in the plastic potential then and the material parameters have to be identified based on the minimization of the error function or solution of a system of equations. Only one reference yield stress appears in the yield condition of Yld2000-2d proposed by Barlat et al. (2003), which predetermines worse predictability of the yield surface shape for various levels of plastic strain when compared to models based on the directional distortional hardening. This especially applies when the flow curves differ substantially with direction. Two aluminium alloys, 6022-T4 and 2090-T3, respectively, were taken from the literature (Barlat et al., 2003) to conduct a study on the influence of flow rule associativity. The material data used for the calibration are summarized in Tab. 1.

The first model here is the associated Yld2000-2d (Barlat et al., 2003), which uses a linear transformation of the stress tensor. The yield function is identical to the plastic potential as

$$f_{Yld2000-2d} = g_{Yld2000-2d} = |X'_1 - X'_2|^m + |2X''_2 + X''_1|^m + |2X''_1 + X''_2|^m - 2\sigma_{ref}^m, \quad (1)$$

where σ_{ref} is the reference yield stress, m is the exponent based on crystal structure (6 for BCC and 8 for FCC) and X'_i and X''_i for $i = 1, 2$ are the principal stresses of linearly transformed stress tensors.

^{*} Ing. Radek Vobejda: Institute of Solid Mechanics, Mechatronics and Biomechanics, Faculty of Mechanical Engineering, Brno University of Technology; Technická 2896/2; 616 69, Brno; CZ, 170387@vutbr.cz

^{**} doc. Ing. František Šebek, Ph.D.: Institute of Solid Mechanics, Mechatronics and Biomechanics, Faculty of Mechanical Engineering, Brno University of Technology; Technická 2896/2; 616 69, Brno; CZ, sebek@fme.vutbr.cz

Tab. 1: Normalized yield stresses and Lankford coefficients (Barlat et al., 2003).

Material	σ_0 [-]	σ_{45} [-]	σ_{90} [-]	σ_{EB} [-]	r_0 [-]	r_{45} [-]	r_{90} [-]	r_{EB} [-]
6022-T4	0.994	0.962	0.948	1.000	0.70	1.48	0.59	1.36
2090-T3	1.000	0.811	0.910	1.035	0.21	1.58	0.69	0.67

The linear transformations of the stress tensor σ are given as $\mathbf{X}' = \mathbf{L}'\sigma$ and $\mathbf{X}'' = \mathbf{L}''\sigma$, where \mathbf{L}' and \mathbf{L}'' are transformation matrices defined as

$$\begin{bmatrix} L'_{11} \\ L'_{12} \\ L'_{21} \\ L'_{22} \\ L'_{66} \end{bmatrix} = \begin{bmatrix} 2/3 & 0 & 0 \\ -1/3 & 0 & 0 \\ 0 & -1/3 & 0 \\ 0 & 2/3 & 0 \\ 0 & 0 & 1 \end{bmatrix} \begin{bmatrix} \alpha_1 \\ \alpha_2 \\ \alpha_7 \end{bmatrix}, \quad \begin{bmatrix} L''_{11} \\ L''_{12} \\ L''_{21} \\ L''_{22} \\ L''_{66} \end{bmatrix} = \frac{1}{9} \begin{bmatrix} -2 & 2 & 8 & -2 & 0 \\ 1 & -4 & -4 & 4 & 0 \\ 4 & -4 & -4 & 1 & 0 \\ -2 & 8 & 2 & -2 & 0 \\ 0 & 0 & 0 & 0 & 9 \end{bmatrix} \begin{bmatrix} \alpha_3 \\ \alpha_4 \\ \alpha_5 \\ \alpha_6 \\ \alpha_8 \end{bmatrix}, \quad (2)$$

where α_j for $j = 1, 2, \dots, 8$ are the independent coefficients, which can be determined based on the minimization of the error function

$$E = \sum_p (\sigma_p^{exp} - \sigma_p^{pre})^2 + \sum_q (r_q^{exp} - r_q^{pre})^2, \quad (3)$$

where p and q are the numbers of yield stresses and Lankford coefficients, respectively, the superscripts *exp* and *pre* are the experimental and predicted values, respectively. In both cases, $m = 8$, since the studied material was aluminium alloy. The resulting independent coefficients are given in Tab. 2.

Tab. 2: Calibrated independent coefficients.

Material	α_1 [-]	α_2 [-]	α_3 [-]	α_4 [-]	α_5 [-]	α_6 [-]	α_7 [-]	α_8 [-]
6022-T4	0.9335	1.0375	0.9329	1.0533	1.0108	0.9350	0.9589	1.1830
2090-T3	0.4963	1.3698	0.7514	1.0252	1.0363	0.9030	1.2306	1.4833

The second model considered was non-associated. The yield function according to Park et al. (2019) is

$$f_{PSY2019} = f(\sigma, \bar{\lambda}) h(\sigma) - 1, \quad (4)$$

where $f(\sigma, \bar{\lambda})$ is the quadratic function according to Stoughton and Yoon (2009), which introduces the anisotropy as

$$f(\sigma, \bar{\lambda}) = \sqrt{\left(\frac{\sigma_{11}}{\sigma_0^2(\bar{\lambda})} - \frac{\sigma_{22}}{\sigma_{90}^2(\bar{\lambda})} \right) (\sigma_{11} - \sigma_{22}) + \frac{\sigma_{11}\sigma_{22} - \sigma_{12}^2}{\sigma_{EB}^2(\bar{\lambda})} + \frac{4\sigma_{12}^2}{\sigma_{45}^2(\bar{\lambda})}}, \quad (5)$$

where σ_{11} , σ_{22} and σ_{12} are the stress tensor components and $\sigma_0(\bar{\lambda})$, $\sigma_{45}(\bar{\lambda})$, $\sigma_{90}(\bar{\lambda})$ and $\sigma_{EB}(\bar{\lambda})$ are the yield stresses defined as functions of plastic multiplier $\bar{\lambda}$. Finally, $h(\sigma)$ introduces the dependency on the Lode angle θ_L as

$$h(\sigma) = \left([C_0 - 1] \left[\frac{2}{\sqrt{3}} \sin\left(\theta_L + \frac{\pi}{3}\right) \right]^4 - 2[C_0 - 1] \left[\frac{2}{\sqrt{3}} \sin\left(\theta_L + \frac{\pi}{3}\right) \right]^2 + C_0 \right)^k, \quad (6)$$

where C_0 is the material parameter and k is the exponent. These were taken $C_0 = 30$ and $k = 0.05$ as reported by Du et al. (2023) for metals with FCC crystal structure.

As mentioned, the widespread function for plastic potential is that proposed by Hill (1948)

$$g_{Hill48} = \sqrt{\sigma_{11}^2 + \lambda_p \sigma_{22}^2 - 2\nu_p \sigma_{11} \sigma_{22} + 2\rho_p \sigma_{12}^2}, \quad (7)$$

where λ_p , ν_p and ρ_p are the functions based on the Lankford coefficients as

$$\lambda_p = \frac{1 + \frac{1}{r_{90}}}{1 + \frac{1}{r_0}}, \quad \nu_p = \frac{1}{1 + \frac{1}{r_0}}, \quad \rho_p = \frac{\frac{1}{r_0} + \frac{1}{r_{90}}}{1 + \frac{1}{r_0}} \frac{1 + 2r_{45}}{2}. \quad (8)$$

3. Comparison of associated and non-associated flow rules

Results for calibrated associated model Yld2000-2d and non-associated one, where the yield function was given by Park et al. (2019) and the plastic potential according to Hill (1948) are depicted in Figs. 1 and 2 for aluminium alloys 6022-T4 and 2090-T3, respectively. The left sides of Figs. 1 and 2 depict the yield stresses and the Lankford coefficients obtained from the tensile tests with 15° angle increment according to the rolling direction together with the values predicted by the respective plasticity models. The right sides of Figs. 1 and 2 show contours of yield functions and plastic potentials for zero shear stress.

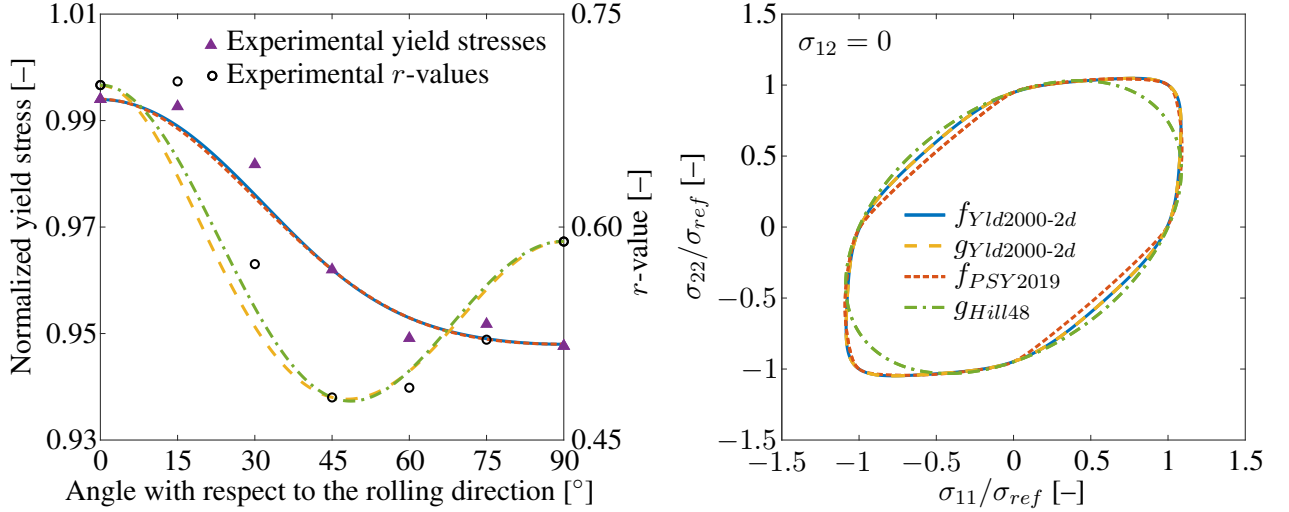


Fig. 1: Results for the aluminium alloy 6062-T4.

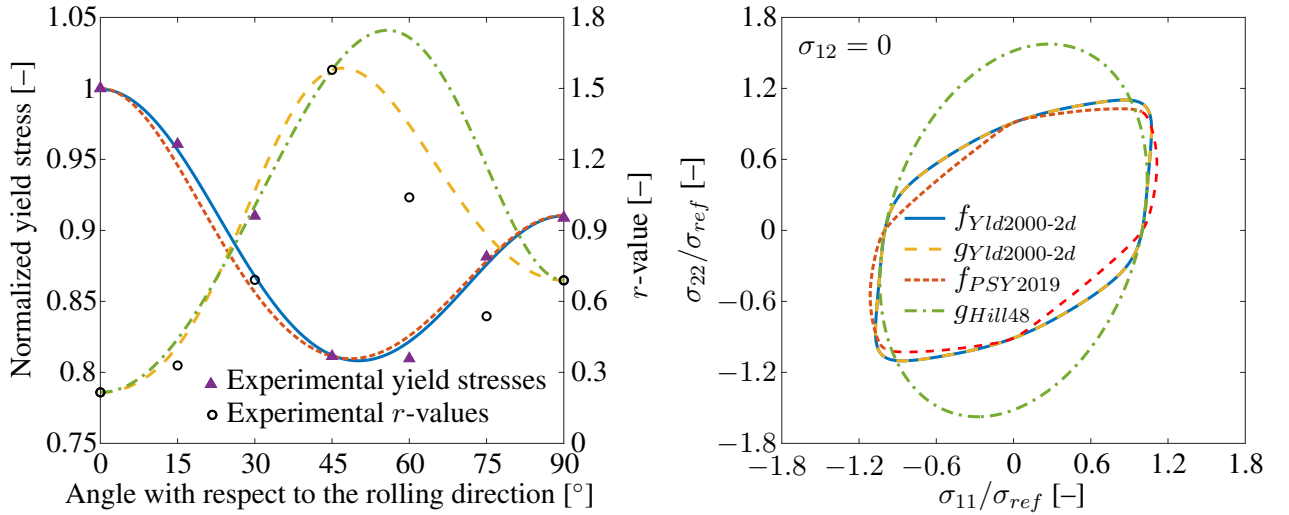


Fig. 2: Results for the aluminium alloy 2090-T3.

The errors in the predicted yield stresses and Lankford coefficients were evaluated for the tensile tests, $E_{y,\phi}$ and $E_{r,\phi}$, respectively, and the equi-biaxial test, $E_{y,EB}$ and $E_{r,EB}$, respectively, as

$$E_{y,\phi} = \sum_n \left| \frac{\sigma_{\phi}^{pre}}{\sigma_{\phi}^{exp}} - 1 \right|, \quad E_{r,\phi} = \sum_n \left| \frac{r_{\phi}^{pre}}{r_{\phi}^{exp}} - 1 \right|, \quad E_{y,EB} = \left| \frac{\sigma_{EB}^{pre}}{\sigma_{EB}^{exp}} - 1 \right|, \quad E_{r,EB} = \left| \frac{r_{EB}^{pre}}{r_{EB}^{exp}} - 1 \right|, \quad (9)$$

where n is the number of directions of the tensile test concerning the angle ϕ according to the rolling. Total errors for yield stresses and Lankford coefficients are $E_y = E_{y,\phi} + E_{y,EB}$ and $E_r = E_{r,\phi} + E_{r,EB}$, respectively. All errors are summarized in Tab. 3.

Tab. 3 clearly shows that the experimental yield stresses were well captured by both plasticity models in the case of minor anisotropy of 6022-T4 aluminium alloy. The associated Yld2000-2d model predicted better the Lankford coefficients as the model was calibrated also from the r -value for the equi-biaxial tension.

Tab. 3: Errors for respective flow rules.

Material	Flow rule	$E_{y,\phi}$ [–]	$E_{y,EB}$ [–]	E_y [–]	$E_{r,\phi}$ [–]	$E_{r,EB}$ [–]	E_r [–]
6022-T4	Associated	0.0164	0.0000	0.0164	0.2648	0.0001	0.2649
	Non-associated	0.0177	0.0000	0.0177	0.2292	0.1276	0.3569
2090-T3	Associated	0.0737	0.0003	0.0740	1.7360	0.0003	1.7363
	Non-associated	0.0979	0.0000	0.0979	2.6252	0.5334	3.1586

Yield stresses and Lankford coefficients were better predicted by the associated Yld2000-2d in general for the highly anisotropic aluminium alloy 2090-T3. It suggests that more sophisticated plastic potential is necessary for highly anisotropic materials. The plastic potential significantly differs from the yield function for this alloy (Fig. 2) than in the case of 6022-T4 (Fig. 1).

The model Yld2000-2d could be formulated using distortional hardening by expressing the independent coefficients α_j for $j = 1, 2, \dots, 8$ as a function of the equivalent plastic strain $\bar{\varepsilon}_p$ (Wang et al., 2009). Then, the yield condition would be better to rewrite as

$$\left(\frac{1}{2} |X'_1 - X'_2|^m + \frac{1}{2} |2X''_2 + X''_1|^m + \frac{1}{2} |2X''_1 + X''_2|^m \right)^{\frac{1}{m}} - 1 = 0, \quad (10)$$

and determine $\alpha_j(\bar{\varepsilon}_p)$ for $j = 1, 2, \dots, 8$ based on optimization at various levels of plastic strain. Otherwise, the results could not be compared with models based on the distortional plasticity theory.

4. Conclusions

The present study focused on the calibration of associated and non-associated models of plasticity for two aluminium alloys, 6022-T4 and 2090-T3, respectively. The total error based on the predicted yield stresses and Lankford coefficients was lower overall for the associated Yld2000-2d model. However, the calibration procedure was done for only one level of plastic strain.

Acknowledgments

This work is an output of the project Computational modelling of ductile fracture of identical wrought and printed metallic materials under ultra-low-cycle fatigue created with financial support from the Czech Science Foundation under the registration no. 23-04724S.

References

- Barlat, F., Brem, J. C., Yoon, J. W., Chung, K., Dick, R. E., Lege, D. J., Pourgoghrat, F., Choi, S. H., Chu, E. (2003) Plane stress yield function for aluminum alloy sheets—part 1: theory. *International Journal of Plasticity*, 19(19), pp. 1297–1319.
- Du, K., Huang, S., Hou, Y., Wang, H., Wang, Y., Zheng, W. and Yuan, X. (2023) Characterization of the asymmetric evolving yield and flow of 6016-T4 aluminum alloy and DP490 steel. *Journal of Materials Science & Technology*, 133, pp. 209–229.
- Hill, R. (1948) A theory of the yielding and plastic flow of anisotropic metals. *Proceedings of the Royal Society of London*, 193(1033), pp. 281–297.
- Min, J., Carsley, J. E., Lin, J., Wen, Y. and Kuhlenkötter, B. (2016) A non-quadratic constitutive model under non-associated flow rule of sheet metals with anisotropic hardening: Modeling and experimental validation. *International Journal of Mechanical Sciences*, 119, pp. 343–359.
- Park, N., Stoughton, T. B. and Yoon, J. W. (2019) A criterion for general description of anisotropic hardening considering strength differential effect with non-associated flow rule. *International Journal of Plasticity*, 121, pp. 76–100.
- Stoughton, T. B. and Yoon, J. W. (2009) Anisotropic hardening and non-associated flow in proportional loading of sheet metals. *International Journal of Plasticity*, 25(9), pp. 1777–1817.
- Wang, H., Wan, M., Wu, X. and Yan, Y. (2009) The equivalent plastic strain-dependent Yld2000-2d yield function and the experimental verification. *Computational Materials Science*, 47(1), pp. 12–22.